

Structure control of poly(p-phenylene vinylene) in layer-by-layer films by deposition on a charged poly(o-methoxyaniline) cushion

Alexandre Marletta, Silésia de Fátima Curcino da Silva, Erick Piovesan, K. R. Campos, Hugo Santos Silva, N. C. de Souza, Maria Letícia Vega, Maria Raposo, Carlos J. L Constantino, Raigna A. Silva, and Osvaldo N. Oliveira Jr.

Citation: *Journal of Applied Physics* **113**, 144509 (2013); doi: 10.1063/1.4798937

View online: <http://dx.doi.org/10.1063/1.4798937>

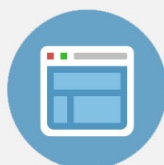
View Table of Contents: <http://scitation.aip.org/content/aip/journal/jap/113/14?ver=pdfcov>

Published by the [AIP Publishing](#)

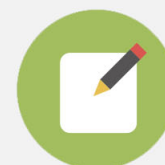


Re-register for Table of Content Alerts

Create a profile.



Sign up today!



Structure control of poly(*p*-phenylene vinylene) in layer-by-layer films by deposition on a charged poly(*o*-methoxyaniline) cushion

Alexandre Marletta,^{1,a)} Silésia de Fátima Curcino da Silva,¹ Erick Piovesan,¹ K. R. Campos,¹ Hugo Santos Silva,¹ N. C. de Souza,² Maria Letícia Vega,³ Maria Raposo,⁴ Carlos J. L. Constantino,⁵ Raigna A. Silva,¹ and Osvaldo N. Oliveira, Jr.⁶

¹Instituto de Física, Universidade Federal de Uberlândia, CP 593, 38400-902 Uberlândia-MG, Brazil

²Grupo de Materiais Nanoestruturados, Campus Universitário do Araguaia, Universidade Federal de Mato Grosso, CEP: 78698-000, Barra do Garças, Mato Grosso, Brazil

³Departamento de Física, Universidade Federal do Piauí, 64049-690 Teresina, PI, Brazil

⁴CEFITEC, Departamento de Física, Faculdade de Ciências e Tecnologia, UNL, Campus de Caparica, 2829-516 Caparica, Portugal

⁵Faculdade de Ciências e Tecnologia, Departamento de Física Química e Biologia, UNESP Universidade Estadual Paulista, 19060-900 Presidente Prudente, SP, Brazil

⁶Instituto de Física de São Carlos, Universidade de São Paulo, CP 369, 13560-970 São Carlos, SP, Brazil

(Received 20 February 2013; accepted 13 March 2013; published online 11 April 2013)

In this paper, we demonstrate that the intrinsic electric field created by a poly(*o*-methoxyaniline) (POMA) cushion layer hinders the changes in molecular conformation of poly(*p*-phenylenevinylene) (PPV) in layer-by-layer with dodecylbenzene sulfonic acid (DBS). This was modeled with density functional theory (DFT) calculations where an energy barrier hampered molecular movements of PPV segments when they were subjected to an electric field comparable to that caused by a charged POMA layer. With restricted changes in molecular conformation, the PPV film exhibited Franck-Condon transitions and the photoexcitation spectra resembled the absorption spectra, in contrast to PPV/DBS films deposited directly on glass, with no POMA cushion. Other effects from the POMA cushion were the reduced number of structural defects, confirmed with Raman spectroscopy, and an enhanced PPV emission at high temperatures (300 K) in comparison with the films on bare glass. The positive effects from the POMA cushion may be exploited for enhanced opto-electronic devices, especially as the intrinsic electric field may assist in separating photoexcited electron-hole pairs in photovoltaic devices.

© 2013 American Institute of Physics. [<http://dx.doi.org/10.1063/1.4798937>]

I. INTRODUCTION

The control of supramolecular architectures is one of the key features exploited in the fabrication of layer-by-layer (LbL) films,¹ which may be considered within the realms of the newly coined area of nanoarchitectonics.² In addition to reaching synergy in the properties of distinct materials in the same film, it is possible to control the characteristics of some layers via direct interaction with the others, as in surface functionalization.² Taking as an example the LbL films from semiconducting polymers, their optical and electrical properties may be tuned by combining with other materials, including fullerenes,³ and carbon nanotubes,⁴ in order to obtain enhanced performance in polymer light emitting diodes (PLEDs),⁵ organic field effect transistors,⁶ and photovoltaic cells.⁷ A widely used luminescent polymer in this regard is poly(*p*-phenylenevinylene) (PPV), the first electroluminescent polymer employed in organic electronics.⁸ Even though the luminescent properties of PPV are inferior to those of other polymers (see a review on luminescent polymers in Ref. 9), it is still useful in fundamental studies, particularly in proof-of-concept type of experiment as it may be processed using various film-forming techniques such as casting, spin-coating, LbL, and Langmuir-Blodgett (LB) methods.

Significantly, the synthesis route to yield PPV using the polymer precursor poly(xilidenotetrahydrothiophenium chloride) (PTHT) already offers opportunities to tune the PPV properties, as the PTHT chorine counter ion may be replaced by dodecylbenzene sulfonic acid (DBS),¹⁰ thus allowing for thermal conversion into PPV in considerably less time and at lower temperatures than in typical conversion procedures.¹¹ Furthermore, with such facile conversion, the number of structural defects arising from oxidative chemical groups (e.g., carbonyl groups) is decreased considerably.

Among the several ways to control the structuring of materials in LbL films is the deposition of the layers on a cushion, for several purposes. The cushion may be used to control surface roughness, to decrease the electrical charge on the surface, to alter interaction with the substrate, or to obtain a layer compatible (or incompatible) with a given type of molecule. Therefore, in choosing the material for the cushion, one has to take into account its charge in solution in addition to the desired final property for the LbL films. In earlier work,⁵ we showed that the operating voltage of PLEDs could be decreased fourfold and the thermal stability of the luminescent properties improved if the PPV LbL films were deposited on a poly(*o*-methoxyaniline) (POMA) cushion. In this paper, we extend the study to investigate possible effects from changing the thickness of the cushion or of the LbL PPV film and explain the origin of the phenomenon leading to the enhanced

^{a)}Author to whom correspondence should be addressed. Electronic mail: marletta@ufu.br. Tel.: +55 34 32394190. Fax: +55 34 32394190.

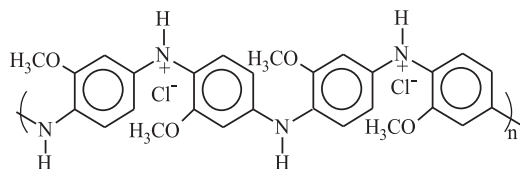


FIG. 1. Chemical formula of poly(o-methoxyaniline) emeraldine salt.

performance. The latter was done with the identification of structural defects from Raman spectroscopy data and with *ab initio* calculations for PPV molecules submitted to an external electric field that controls their molecular conformation.

II. METHODOLOGIES

Figure 1 shows the chemical structure of POMA in the salt emeraldine form, which is water soluble and used in the preparation of LbL films. Details of the POMA synthesis and deposition processes can be found in Ref. 12. Aqueous solutions were obtained by dissolving 0.0615 g of POMA in acetonitrile and then in ultrapure water (Milli-Q) (acetonitrile/water (1 ml:49 ml)). The solution was kept in an ultrasound bath during 1 h. After 2 h at rest, the solution was filtered with a 25–50 μm porosity filter because POMA is not completely soluble in acetonitrile and water. The concentration of the filtered solution was estimated at 0.6 g l⁻¹ by measuring the ultraviolet-visible spectrum of the solution and using the calibration procedure established in Ref. 12.

The semiconducting polymer PPV shown in Fig. 2(c) is commonly obtained by thermal conversion of a non-conjugated polymer precursor, PTHT (Fig. 2(a)), through the elimination of the PTHT lateral group via thermal treatment at high temperatures (200 °C) for long periods of time (6 h) in vacuum. The thermal conversion introduces structural defects due to thermal oxidation, such as carbonyl groups (C=O), which reduce the effective conjugation length and behave as photoquenching centers, leading to a decreased quantum efficiency for luminescence. This problem can be alleviated by using an alternative method¹⁰ where conversion may take place at low temperatures (around 110 °C), within short periods of time (~3 min) and in air. This route consists in the partial substitution of the Cl⁻ counter-ion of PTHT with dodecylbenzene sulfonic acid (DBS) ions, as indicated in Fig. 2(b).

The substrates used were BK7 glass slides (1 × 2 cm²) washed initially with water and detergent. To obtain

hydrophobic substrates, the BK7 slides were washed using the RCA procedure,¹³ i.e., with a solution containing hydrogen peroxide (H₂O₂) and sulfuric acid (H₂SO₄) in a 3:7 ratio, during 1 h in an ultrasound bath. Then, the substrates were rinsed with ultrapure water and immersed in a solution with ultrapure water (Milli Q), hydrogen peroxide (H₂O₂), and ammonium hydroxide (NH₄OH) in the volume ratio of 5:1:1, for 30 min in an ultrasound bath. Finally, the substrates were rinsed in ultrapure water.

The LbL films of POMA-PTHT/DBS were deposited onto BK7 substrates by immersing the substrates for 2 min in a solution of POMA, with concentration of 0.6 g l⁻¹, and subsequent drying with N₂. This procedure was repeated several times to obtain the number of desired layers of POMA. Note that multiple layers of POMA can be deposited on the same substrate, without alternating with layers of another material, because POMA adsorption may occur via secondary interactions, such as H-bonding, in addition to electrostatic interactions.¹⁴ The substrates coated with POMA LbL films were alternately immersed in a 0.3 mg ml⁻¹ PTHT solution and a 0.1 mol l⁻¹, pH = 5 DBS solution. The immersion time of the substrate in the POMA solution was 1 min, while it was 30 s for PTHT and DBS solutions. This procedure was repeated to get the number of PTHT/DBS bilayers desired. Finally, conversion into PPV was achieved via thermal treatment at high and low temperatures under vacuum (10⁻¹ atm) for 2 h, thus leading to the architecture BK7/POMA-PPV/DBS LbL films. For the sake of clarity, the samples are referred to by using the label A_{XXX}Y_{YY}Z_{ZZ}, where XXX is the thermal conversion temperature (TC), i.e., 110 °C or 230 °C; YY is the number of POMA layers: 00, 02, 05, 10, and 20, and ZZ is the number of PPV/DBS bilayers: 05, 25, and 50.

Linear absorption measurements were performed using a Shimadzu UV-Vis spectrometer model UV-160, under room conditions, in the range between 350 and 1000 nm. Photoluminescence (PL) measurements for various sample temperatures (16–300 K) were performed using a He closed cycle cryostat under vacuum (1.3 × 10⁻² mbar) and the 458 nm line of an Ar⁺ laser with average excitation of 5 nW cm⁻². The detection system was mounted using a photomultiplier on a 0.5 m monochromator for detection in the lock in mode. The ambient photoluminescence excitation (PLE) was performed in a spectrometer Hitachi F-450. Raman spectroscopy measurements were performed using a micro-Raman Spectrograph RENISHAW model in-Via, using a 785 nm

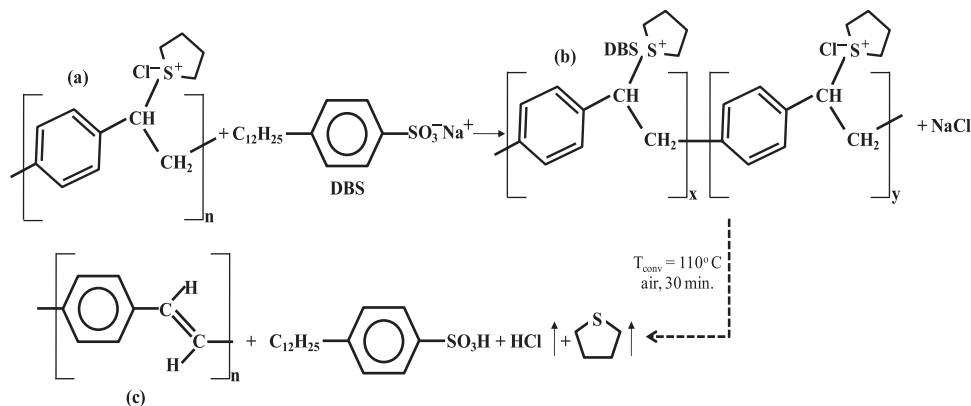


FIG. 2. Thermal conversion of PTHT (a) into PPV (c), through the alternative route (b) using DBS as counter ion.

laser, grating with 1200 lines/mm and a 50 \times objective lens with a focal length of ca. 0.3 μ m.

As for the theoretical calculations, the geometry of the PPV ground state with 3 monomers in the gaseous state was determined by Density Functional Theory (DFT). The ground state formulation was based on functional hybrid B3LYP exchange and correlation, with Gaussian 6–31G** in the Orca 2.9 package. Starting from the molecule geometry, a super-unit cell was chosen and then the torsion between adjacent monomers was obtained without allowing for structural relaxation. With periodic boundary conditions applied, the dependence of total energy with and without the electric field bias was studied in the package Siesta 3.1, based on DZP and functional exchange and correlation GGA-PBE.

III. RESULTS AND DISCUSSION

A. Effects from the POMA cushion

The formation of PPV/DBS LbL films on a POMA cushion leads to optical absorption features characteristic of a PPV film, with some modifications caused by absorption of POMA. Figure 3 shows the absorption spectra of POMA-PPV/DBS LbL films with various numbers of bilayers and thermally converted at 110 and 230 $^{\circ}$ C, where the spectra were shifted in the y-axis to facilitate visualization. For films converted at low temperature (110 $^{\circ}$ C) in Figure 3(a), the first band at \sim 445 nm is assigned to transitions from delocalized states of PPV and POMA conjugated segments, while the second one is the POMA polaronic band centered at \sim 800 nm.¹⁰ No absorption is expected from DBS, which absorbs from 180 to 350 nm.¹⁰ The absorption of the first band increased with the number of PPV/DBS layers deposited, as expected. The conversion temperature did not affect the band assigned to PPV in the POMA-PPV/DBS LbL films, with the spectra in Figure 3(b) exhibiting essentially the same features as in Figure 3(a). On the other hand, the POMA polaronic band was red shifted for 25 and 50-bilayer PPV/DBS LbL films converted at the lower temperature (110 $^{\circ}$ C). This is due to the elimination of HCl or DBS species during PPV conversion

process, which then diffuse to the POMA-PPV interface and co-dope the POMA layer.⁵ The polaronic band was less defined and blue shifted for the higher thermal conversion temperature (230 $^{\circ}$ C), as seen in Figure 3(b), because polymer degradation is expected to increase above 150 $^{\circ}$ C.¹⁰

Figures 3(c) and 3(d) display the maximum of the absorbance intensity of POMA + PPV $\pi \rightarrow \pi^*$ band ($<$ 500 nm) as a function of the number of PPV/DBS bilayers. Since the absorbance spectra between 350 and 500 nm can be described by $A = A_{\text{POMA}} + A_{\text{PPV}}$, where A_{POMA} and A_{PPV} are the absorbance of POMA and PPV, respectively, for a fixed number of POMA layers the adsorption rate for PHTT/DBS may be obtained from the slope $\frac{dA_{\text{PPV}}}{dN} \approx \frac{dA}{dN} |_{A_{\text{POMA}}}$. Figures 3(c) and 3(d) show an almost constant slope, $\frac{dA_{\text{PPV}}}{dN} \approx 10^{-3}$, regardless of the number of POMA layers. Furthermore, the adsorption rate is preserved after the PPV conversion procedure. The amount of material adsorbed per layer is comparable to that for PPV/DBS bilayers deposited on glass substrates.^{14,15}

A drastic improvement is seen in thermal stability of emission properties when the POMA cushion is used for deposition of PPV/DBS films, regardless of the thermal conversion temperature. Figures 4(a) and 4(b) illustrate this finding with the emission spectra obtained at various temperatures, from 16 to 300 K, for samples A2300225 (with a 2-layer POMA cushion) and A2300025 (no cushion), respectively. Figure 4(c) shows the temperature dependence for the integrated area of the spectra (normalized to unity for 16 K) for all samples, from which one can infer a decrease of 80% in emission when the temperature is increased for the film without POMA cushion. In contrast, the decrease is much less for the PPV/DBS LbL films adsorbed on the POMA cushion. For the latter, the PL line shape and peak positions were essentially the same for all samples, regardless of the POMA or PPV/DBS thickness or conversion temperature. An electronic transition appears at \sim 517 nm with phonon first and second replica at \sim 555 nm and \sim 600 nm, respectively. For the higher thermal conversion temperature, there is a small band broadening and blue shift (\sim 5 nm), probably because the film was more structurally disordered due to structural

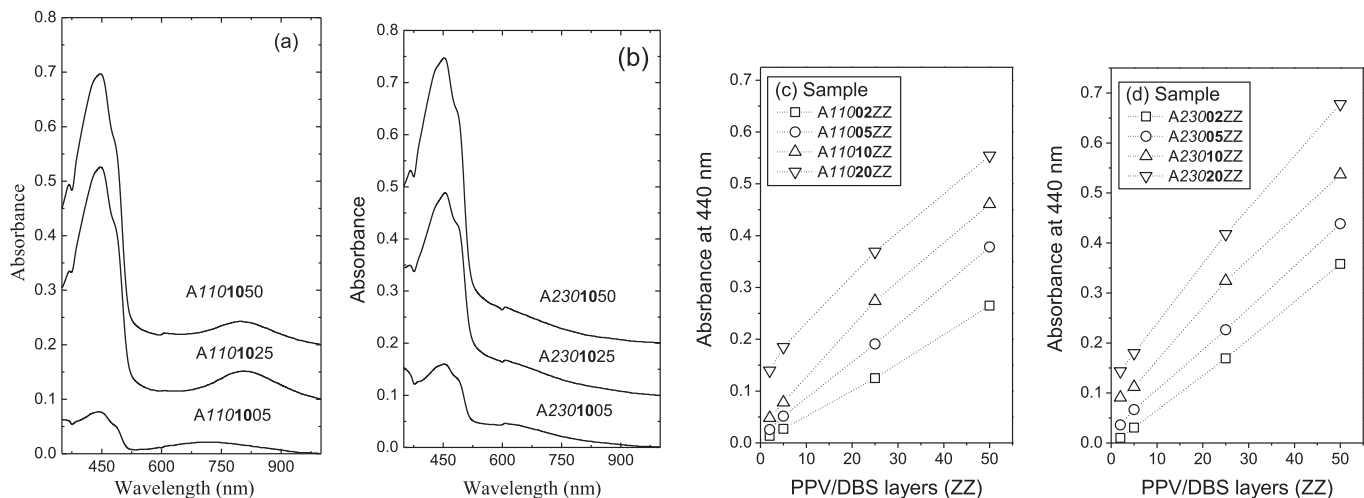


FIG. 3. Linear absorption spectra of POMA-PPV/DBS films converted at (a) 110 $^{\circ}$ C and (b) 230 $^{\circ}$ C for POMA layers $YY = 10$ and PPV/DBS bilayers $ZZ = 05, 25,$ and 50 . Absorbance intensity at 440 nm as a function of the number of layers of PPV/DBS bilayers for films converted at 110 $^{\circ}$ C (c) and 230 $^{\circ}$ C (d). The dashed lines are just to guide the eyes.

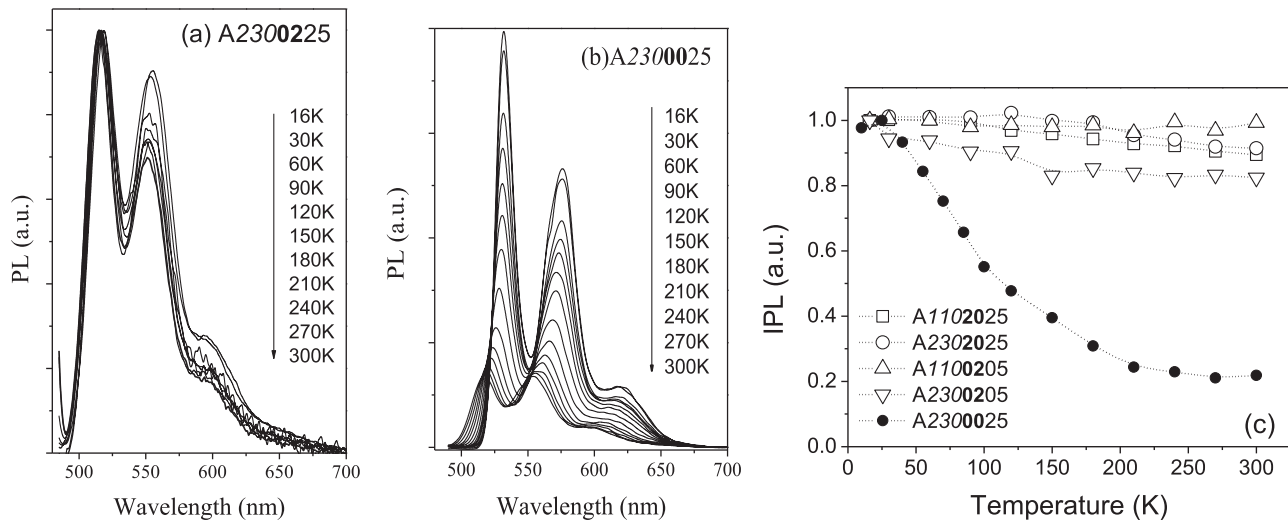


FIG. 4. Temperature dependence of photoluminescence spectra of LbL POMA-PPV/DBS films: (a) A2300225 and (b) A2300025. (c) Temperature dependence of the integrated photoluminescence for samples A1102025, A2302025, A110205, A2300205, and A2300025.

defects, such as carbonyl groups, as the PPV glass transition temperature (T_g) is ~ 200 °C.¹⁶ For the PPV/DBS LbL films deposited on glass substrates (no cushion), the PL spectra were shifted by 15 nm in addition to the decrease in intensity.⁶

In summary, the quenching channels activated at high temperatures are eliminated, so that PPV films display an almost temperature-independent PL. This inactivation of quenching channels is related to elimination of carbonyl defects, as will be proven with Raman spectroscopy later on. In subsidiary experiments, we observed that this inactivation does not depend on the thickness of the POMA cushion or on the conversion temperature (see supplementary material).¹⁷

The vibrational transition probabilities were not affected by the increase in temperature for the POMA-PPV/DBS LbL films, again in contrast to the PPV/DBS film without cushion. This is shown in Table I which brings the Huang-Rhys factor, S , for all samples. This factor was calculated by fitting the emission spectra with multi-Gaussians curves (results not shown here), in order to obtain the peak position, the full width at half-maximum (FWHM), and peak area, as follows:

$$S \approx \frac{A_2 \omega_1}{A_1 \omega_2}, \quad (1)$$

where A_i and ω_i correspond to the area and width of the peaks, respectively, and taking $i = 1$ for the peak associated with the zero phonon (517 nm) and $i = 2$ for the first vibrational mode (555 nm). In these calculations, the emission spectra were corrected with the self-absorption factor. The slightly larger S for samples converted at the higher temperature is probably due to the increase in structural defects.¹⁷

TABLE I. Huang-Rhys factor obtained from emission spectra of POMA-PPV/DBS LbL films obtained at 16 and 300 K.

Sample	A1100505	A2300505	A1102025	A2302025	A2300025
S (T = 300 K)	0.62	0.66	0.78	0.82	0.92
S (T = 16 K)	0.60	0.61	0.76	0.79	0.78

It has been suggested that the enhanced emission properties in PPV/DBS LbL films brought by the introduction of a POMA cushion on top of the glass substrate could be associated with a smaller number of structural defects.¹⁸ Here, we used Raman spectroscopy to confirm this expectation. Figure 5 shows that the scattering intensity near 1690 cm^{-1} , associated with carbonyl groups (structural defects), is practically the same for all PPV/DBS LbL films deposited on a POMA cushion with different thicknesses, even though the conversion temperature differed. This is in contrast to PPV/DBS LbL films deposited on glass and converted at a high temperature (230 °C), which exhibited a larger band in comparison to the film converted at 110 °C.¹⁸ Therefore, separating the PPV/DBS bilayers from the substrate with POMA layers indeed reduces the structural defects significantly, consistent with the PL result in Figure 4(c) that is independent of the sample preparation conditions.

The band assignment for Figure 5 is as follows:¹⁹ C-O-C and the symmetric modes of SO_3 anion at 1171 cm^{-1} ; C-C of vinyl group at $\sim 1390\text{ cm}^{-1}$, C=C from benzene ring at $\sim 1550\text{ cm}^{-1}$ and at 1584 cm^{-1} , and C-C at 1629 cm^{-1} . The band at $\sim 577\text{ cm}^{-1}$ is assigned to the in-plane deformation of the benzene ring amine and the band at $\sim 1356\text{ cm}^{-1}$ is related to the ion radical in emeraldine salt POMA. The bands for samples converted at 230 °C (Figures 5(c) and 5(d)) normally have larger width at half maximum than for the films converted at 110 °C (Figures 5(a) and 5(b)). This is caused by the greater structural disorder with the high conversion temperature above the PPV glass transition temperature, ~ 200 °C, again in agreement with the small PL broadening in Figure 4. The Raman spectra are practically independent of the number of PPV layers in the film. Taking into account the emission spectra in Figure 4, one can also identify the optical active vibrational mode for PPV emission. The energy difference between the zero emission and first phonon replica is 168 meV ($\sim 1360\text{ cm}^{-1}$). Comparing with the values for the Raman bands, the mode optically active is the vinyl C-C group.

We have also found that the PLE spectra resemble the absorbance spectra for POMA-PPV/DBS LbL films, as

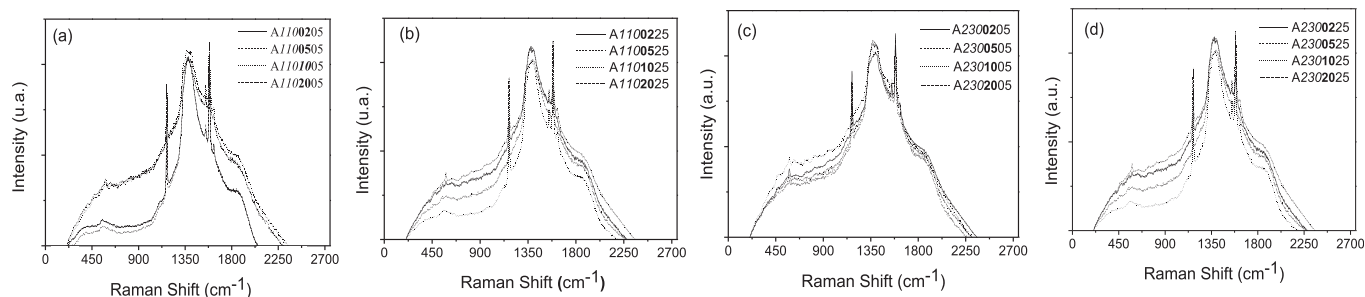


FIG. 5. Raman spectra recorded with the 785 nm laser line for POMA-PPV/DBS LbL films prepared under different conditions: (a) A1100205, A1100505, A1101005, and A1102005, (b) A1100225, A1100525, A1101025, and A1102025, (c) A2300205, A2300505, A2301005, and A2302005, and (d) A2300225, A2300525, A2301025, and A2302025.

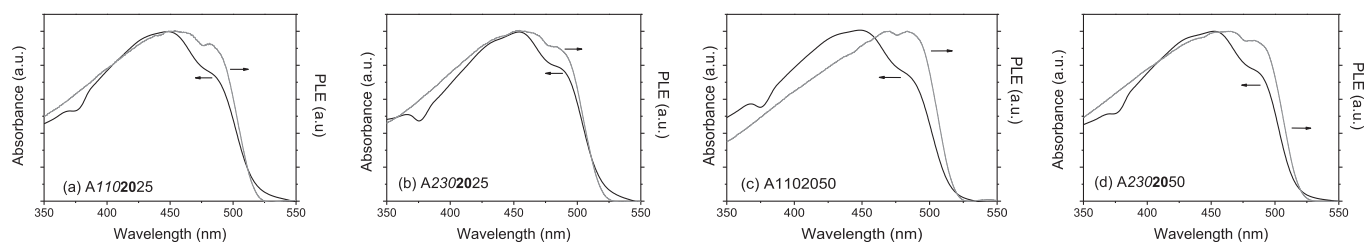


FIG. 6. Normalized absorbance and excitation spectra in the UV-Vis region for POMA-PPV/DBS LbL films with (i) 2 POMA layers and 25 PPV/DBS layers thermally converted at 110 °C (a) and at 230 °C (b), and (ii) 20 POMA layers and 50 PPV/DBS layers thermally converted at 110 °C (c) and at 230 °C (d).

indicated in Figure 6 depicting the normalized spectra for samples converted at the two temperatures used. The excitation spectra were obtained by fixing the detection wavelength, λ_D , at the maximum of emission band for the first phonon replica, $\lambda_D = 555$ nm. Therefore, with the POMA cushion, the thermal treatment for conversion into PPV is not sufficient to change the conformation of the PPV polymer chains, in contrast to PPV/DBS films deposited on bare glass.⁵ The electronic transitions in Figure 6 should be considered as Franck-Condon type, with the PPV conformation in the excited state being the same as in the ground state, which differs from the results for PPV films deposited on glass where the photoexcitation spectra are considerably different from the absorbance spectra.⁵

Having observed the effects introduced by the POMA cushion above, we verified whether other properties of PPV/DBS LbL films had been affected. We noted that other properties of PPV films are maintained, and this is shown in the supplementary material. For instance, there is anisotropy in the PL spectra, with higher intensity in the dipping direction. The presence of POMA layer does not interfere with the nanostructuring of the PPV film, as demonstrated in AFM images (treated with statistical methods). Again this occurs regardless of the thickness of POMA layer and conversion temperature.

B. Theoretical model

The main effects caused by the POMA cushion were the reduction of the number of structural defects and the hindering of changes in molecular conformation for PPV molecules. The obvious origin for the second effect should be the intermolecular interactions between charged POMA molecules and PPV, but this is not easily modeled for one does

not know the molecular conformations in detail. In a simplified model for such interactions, we consider the conformation of PPV chains under an external electric field that should mimic the charged POMA layer. The energy of the ground state for a PPV chain was calculated with the Density Functional Theory. The unidirectional electric field was applied perpendicular to the plane defined by the backbone phenylene rings, in the no-torsion situation. Periodic boundary conditions were assumed and the chain was taken as isolated with no interaction with neighboring chains. Torsion was defined between two next-neighbor phenylene rings along the polymer main chain, owing to the choice of a unit cell with periodic boundary conditions. The magnitude of the applied field varied between 0 and 1 eV/Å along the z direction, with the polymer chain being located on the xy

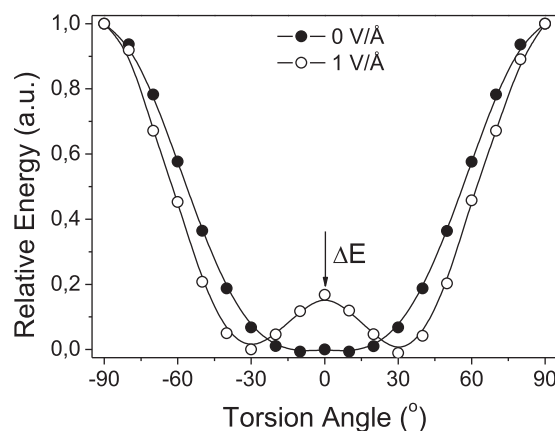


FIG. 7. Relative energy in function of torsion angle between adjacent PPV monomers under the influence of an external static electric field, 0 V/Å (close circles) and 1 V/Å (open circles).

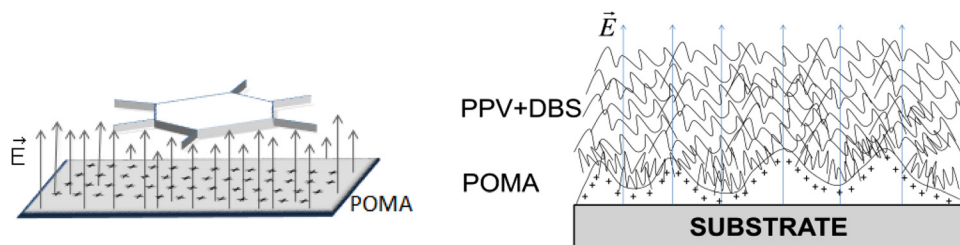


FIG. 8. Illustrative scheme of a POMA-PPV/DBS LbL film and the electric field \vec{E} associated with the surface charge on the POMA layer.

plane. The zero reference energy per unit cell is taken for the case where the PPV molecule is totally planar.

The magnitude of the applied field was estimated as follows. The potential energy difference due to the POMA layer should be at most 0.1 eV for a 100 nm-PPV film, considering a parallel-plate capacitor model and a surface charge density of 5 C/m^2 estimated from XPS measurements that demonstrated the existence of excess surface charge.^{20,21} Each PPV segment is under a potential energy difference of 0.6 eV, estimated by taking a dielectric constant of 3 for a conjugated polymer ($\epsilon = 3\epsilon_0$)²² and a typical width of a segment of 5 Å. This energy difference of 0.6 eV is consistent with the experimentally obtained activation energy (0.651 eV) for a full rotation of the phenyl ring of crystalline PPV measured with nuclear magnetic resonance (NMR).²³ It is also comparable with the energy required to rotate the ring at 90 °C obtained from the torsion potential using the density functional theory (0.560 eV).²⁴ These experimental and theoretical values were confirmed using Solid-State MAS-Exchange NMR Exchange techniques.²⁵

Figure 7 shows two curves of relative energy as a function of the relative torsion angle between adjacent PPV monomers. When no field is applied, there is just one broad minimum centered at 0°, in agreement with Capaz and Caldas.²⁴ If the field is applied, however, a configurational energy barrier ΔE appears, also centered at 0°. Thus, the minimal configurational energy occurs at $\pm 30^\circ$ owing to the electric field. The appearance of this barrier, which amounts to a hindering for changes in molecular conformation for the PPV chains, is capable of explaining the various experimental findings for the POMA-PPV/DBS LbL films (Fig. 8). First, the photoluminescence spectra at 16 K of POMA-PPV/DBS LbL films are blue shifted in comparison to those of PPV/DBS films deposited on glass because the molecular torsion decreases the effective conjugation degree of PPV segments in the presence of the POMA layer⁵ (i.e., with the applied electric field in our model). Second, the energy barrier at 0° accounts for the smaller blue-shift in PPV emission ($\sim 5 \text{ nm}$) than the $\sim 15\text{--}20 \text{ nm}$ shift observed for the film without POMA¹⁸ when the sample temperature increased from 16 to 300 K. Finally, with the POMA layer, the PPV/DBS LbL films exhibit an almost temperature independent PL for two reasons: (i) there are less structural defects, as demonstrated with Raman spectroscopy; (ii) because changes in molecular conformation are hindered, less active vibration states will be available for energy transfer, and non-radiative channels are reduced considerably.

IV. CONCLUSIONS

With a systematic study of the optical and structural properties of POMA-PPV/DBS LbL films, we could confirm that a

POMA cushion brings a number of welcome features for the film properties. These include a smaller number of structural defects and the observation of an almost temperature-independent PL spectrum, since with the POMA cushion the emission did not decrease considerably when the temperature was increased. These effects are observed for distinct thicknesses of the POMA cushion and for PPV/DBS LbL films containing different numbers of bilayers. The smaller number of structural defects was probed with Raman spectroscopy while the inactivation of non-radiative channels caused by POMA could be explained by a simple model, where PPV chains were subjected to an electric field simulating the POMA surface charges. Indeed, according to DFT calculations for isolated PPV segments, the application of a static electric field generates an energy barrier that is consistent with decreased degrees of molecular freedom. Changes in molecular conformation were then hindered, thus making electronic-vibrational states less available for energy transfer, consistent with the experimentally observed behavior for PPV emission.

We suggest that the positive effects from the POMA cushion can be exploited in the design of opto-electronic devices with less oxidation-related defects, high emission efficiency, and enhanced thermal stability. The intrinsic potential difference of ca. 1 eV/\AA arising from POMA surface charge, for example, can be used in separating photoexcited electron-hole pairs in multilayer structures for photovoltaic devices. Furthermore, we have also demonstrated that DFT calculations may be useful to probe models devised to explain optical properties of nanostructured films.

ACKNOWLEDGMENTS

The authors acknowledge the Brazilian financial support from CNPq, CAPES, FAPEMIG, FAPESP, and INEO/MCT, in addition to the bilateral program CAPES-Brazil/Grices-Portugal. We are thankful to Professor Dr. Reinaldo Ruggiero, Federal University of Uberlândia, Minas Gerais, Brazil, for the use of experimental facilities.

¹K. Ariga, Q. Ji, J. P. Hill, Y. Bando, and M. Aono, *NPG Asia Mater.* **4**, e17 (2012).

²K. Ariga, A. Vinu, Y. Yamauchi, Q. Ji, and J. P. Hill, *Bull. Chem. Soc. Jpn.* **85**, 1 (2012).

³H. Li and W. Jizheng, *Appl. Phys. Lett.* **101**, 263901 (2012).

⁴J.-B. Sim, H.-H. Yang, M.-J. Lee, J.-B. Yoon, and S.-M. Choi, *Appl. Phys. A* **108**, 305 (2012).

⁵A. Marletta, E. Piovesan, N. O. Dantas, N. C. de Souza, C. A. Olivati, D. T. Balogh, R. M. Faria, and O. N. Oliveira, Jr., *J. Appl. Phys.* **94**, 5592 (2003).

⁶S. Ju, K. Lee, D. B. Janes, M.-H. Yoon, A. Facchetti, and T. J. Marks, *Nano Lett.* **5**, 2281 (2005).

⁷M. Ogawa, M. Tamanoi, H. Ohkita, H. Benten, and S. Ito, *Sol. Energy Mater. Sol. Cells* **93**, 369 (2009).

- ⁸J. H. Burroughes, D. D. C. Bradley, A. R. Brown, R. N. Marks, K. Mackay, R. H. Friend, P. L. Burns, and A. B. Holmes, *Nature* **347**, 539 (1990).
- ⁹L. Akcelrud, *Prog. Polym. Sci.* **28**, 875 (2003).
- ¹⁰A. Marletta, D. Gonçalves, O. N. Oliveira, Jr., R. M. Faria, and F. E. G. Guimaraes, *Adv. Mater.* **12**(1), 69 (2000).
- ¹¹D. D. C. Bradley, *J. Phys. D: Appl. Phys.* **20**, 1389 (1987).
- ¹²M. Raposo, L. H. C. Mattoso, and O. N. Oliveira, Jr., *Thin Sol. Films* **327–329**, 739 (1998).
- ¹³W. Kern, *Semicond. Int.* **7**(4), 94 (1984).
- ¹⁴A. Marletta, R. A. Silva, P. A. Ribeiro, M. Raposo, and D. Gonçalves, *Langmuir* **25**, 2166 (2009).
- ¹⁵A. Marletta, R. A. Silva, P. A. Ribeiro, M. Raposo, and D. Gonçalves, *J. Non-Cryst. Solids* **354**, 4856 (2008).
- ¹⁶D. Rakovic, R. Kostic, L. A. Gribov, and I. E. Davidova, *Phys. Rev. B* **41**, 10744 (1990).
- ¹⁷See supplementary material at <http://dx.doi.org/10.1063/1.4798937> for analysis of the molecular order in LbL POMA-PPV/DBS films confirmed using data from polarized absorbance and emission, and Atomic Force Microscopy topology images.
- ¹⁸E. M. Therézio, E. Piovesan, M. Anni, R. A. Silva, O. N. Oliveira, Jr., and A. Marletta, *J. Appl. Phys.* **110**, 044504 (2011).
- ¹⁹K. F. Voss, C. M. Foster, L. Smilowitz, D. Mihailović, S. Askari, G. Srdanov, Z. Ni, S. Shi, A. J. Heeger, and F. Wudl, *Phys. Rev. B* **43**, 5109 (1991).
- ²⁰J. M. C. Lourenço, P. A. Ribeiro, A. M. Botelho do Rego, and M. Raposo, *J. Colloid Interface Sci.* **313**, 26 (2007).
- ²¹M. Raposo, J. M. C. Lourenço, A. M. B. do Rego, A. M. Ferraria, and P. A. Ribeiro, *Colloids Surf., A* **412**, 1 (2012).
- ²²M. Tammer and A. P. Monkman, *Adv. Mater.* **14**(3), 210 (2002).
- ²³J. H. Simpson, D. M. Rice, and F. R. Karasz, *J. Polym. Sci., Part B: Polym. Phys.* **30**, 11 (1992).
- ²⁴R. B. Capaz and M. J. Caldas, *Phys. Rev. B* **67**, 205205 (2003).
- ²⁵E. R. de Azevedo, R. W. A. Franco, A. Marletta, R. M. Faria, and T. J. Bonagamba, *J. Chem. Phys.* **119**, 2923 (2003).